

Neuro-Symbolic Generation of Explanations for Robot Policies with Weighted Signal Temporal Logic

Mikihisa Yuasa¹, Ramavarapu S. Sreenivas¹, Huy T. Tran¹

Abstract—Learning-based policies have demonstrated success in many robotic applications, but often lack explainability, which poses challenges in safety-critical deployments. To address this, we propose a neuro-symbolic explanation framework that generates a weighted signal temporal logic (wSTL) specification which describes a robot policy in a human-interpretable form. Existing methods typically produce explanations that are verbose and inconsistent, which hinders explainability, and loose, which limits meaningful insights into the underlying policy. We address these issues by introducing a simplification process consisting of predicate filtering, regularization, and iterative pruning. We also introduce three novel explainability evaluation metrics—conciseness, consistency, and strictness—to assess explanation quality beyond conventional classification metrics. Our method is validated in three simulated robotic environments, where it outperforms baselines in generating concise, consistent, and strict wSTL explanations without sacrificing classification accuracy. This work bridges policy learning with explainability through formal methods, contributing to safer and more transparent decision-making in robotics.

I. INTRODUCTION

Recent innovations in learning-based methods, particularly those using neural networks, have significantly improved both high-level decision-making and low-level control in robotics. However, these neural network policies are inherently black-box in nature, which poses significant concerns for safety-critical robotic applications, such as autonomous vehicles, where explainability is paramount. To address these concerns, various approaches have been explored to enhance explainability of learned policies [1], [2], including post-hoc analysis techniques [3], [4] and methods to learn policies that are inherently explainable [5], [6].

In this paper, we focus on post-hoc analysis to enable explanation of any given robot policy. While existing approaches, like saliency maps [7] and feature attribution [8], provide valuable information, they often lack language-based explanations, which limits human-interpretability. Autoregressive language models have recently shown promising results for providing language-based explanations [9]–[11], but they do not support formal verification of the output explanation, which limits their applicability in domains requiring strong safety and correctness assurances [12].

Formal methods offer an alternative that emphasizes verifiability. In particular, temporal logic has been used to specify robotic tasks and system constraints in an interpretable yet

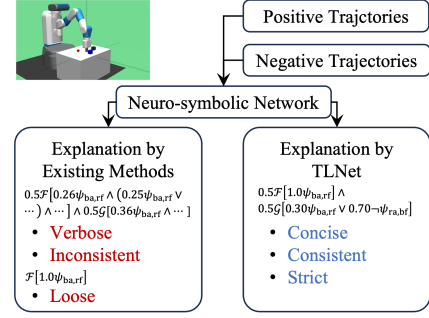


Fig. 1. Existing methods for neuro-symbolic post-hoc explainability produce specifications that are verbose (i.e., include unnecessary predicates), inconsistent across training seeds, and loose (e.g., “catch-all” specifications that do not provide useful insights). Our proposed network, TLNET, addresses these concerns.

mathematically precise manner that supports verification [13]–[15]. Recent efforts have also used temporal logic, primarily linear temporal logic (LTL) and signal temporal logic (STL), to infer explanations of given trajectory data. For example, [16]–[18] use a decision tree classifier to infer the LTL or STL specification that best explains the difference between two classes of trajectories. [19] uses a greedy explanation search method over explanation candidates in LTL driven by policy similarity metrics. However, these methods are limited in their ability to infer specifications where certain predicates are more critical than others. For instance, [18] can infer such relations only for conjunctions. *Weighted signal temporal logic* (wSTL) [20] extends LTL and STL by introducing importance weights over predicates, which can highlight the relative priority of various task components. The expressiveness of wSTL thus makes it particularly suitable for describing robotic behaviors in settings with competing or hierarchical objectives.

The presence of real-valued weights in wSTL has enabled the use of neural network approaches for inferring wSTL specifications that explain given trajectory data. These methods have shown promising results, where they show high classification performance for various applications, including anomaly detection in naval surveillance [21], fault diagnosis [22], and weather forecasting [23]. However, existing work only focuses on classification accuracy, which does not fully capture the actual explainability of learned specifications. For example, as shown in Figure 1, these methods often produce specifications that are unnecessarily verbose (i.e., they include many unnecessary predicates), inconsistent across seeds, and/or loose, such that they are satisfied but do not

¹The Grainger College of Engineering, University of Illinois Urbana-Champaign, Urbana, IL 61801 USA. {myuasa2, rsree, huytran1}@illinois.edu

*This work was supported in part by the Office of Naval Research (ONR) under Grant N00014-20-12249 and JASSO Study Abroad Fellowship Program (Graduate Degree Program).

provide useful insights (e.g., “catch-all” specifications that include many conjunctions or overly simplified specifications that do not fully capture the task or constraints). Some works address verbosity by incorporating heuristic simplification methods, like only keeping the top- k weighted predicates [21], [24] or using a greedy process to remove weights [25]. However, as we show in our empirical results, no existing methods effectively balance classification accuracy with verbosity, inconsistency, and looseness.

In this work, we propose TLNET, a neural network architecture for inferring wSTL explanations of robot policies that are concise (i.e., include as few predicates as needed), consistent (i.e., produce similar explanations across training seeds), and strict (i.e., contain as few disjunctions as needed). Our method targets a subclass of wSTL structures with arbitrary conjunctions and disjunctions of predicates in temporal clauses. TLNET includes a multi-step simplification process that reduces specification verbosity and improves consistency, while ensuring strictness is maintained. This process includes a predicate filtering step, a regularized loss function, and iterative weight pruning. We also provide theoretical justification for our wSTL-based neural network architecture, which essentially reduces learning parameters by the distributivity of importance weight, and introduce novel metrics for quantifying explainability—conciseness, consistency, and strictness—that complement standard classification accuracy, addressing a significant gap in current evaluation practices. We demonstrate our method in three simulated robotics environments that vary in continuity, dimensionality, task structure, and policy complexity, and show that it generally outperforms baselines with respect to classification accuracy and our proposed explainability metrics. TLNET bridges the gap between neural network-based policy learning and provides formal explanations of learned policies, offering a step toward safer and more transparent robotic systems.

II. PRELIMINARIES

Let a trajectory (or a signal) of n -dimensional states be a discrete-time series $\tau = s_0, s_1, \dots, s_H$, where $s_t \in S$ is a state at timestep $t \in \mathbb{Z}_{>0}$, $S \subseteq \mathbb{R}^n$ is the state space, and H is the time horizon of τ . We also define an interval I as $I := [a, b] = \{k \in \mathbb{Z}_{>0} | a \leq k \leq b; a, b \in \mathbb{Z}_{>0}\}$, $|I|$ as the cardinality of I , and $t + I$ as the interval $[t + a, t + b]$.

A. Weighted Signal Temporal Logic

We consider wSTL syntax [20] defined recursively as $\phi := \top \mid \psi \mid \neg\phi \mid \bigwedge_{i=1}^N w\phi_i \mid \bigvee_{i=1}^N w\phi_i \mid \mathcal{G}_I^w\phi \mid \mathcal{F}_I^w\phi$, where \top is the logical *True* value, $\psi := f(s) \geq c$ is an atomic predicate given a function $f : S \rightarrow \mathbb{R}$ with constant $c \in \mathbb{R}$, and \neg , \wedge , and \vee are Boolean *negation*, *conjunction*, and *disjunction* operators, respectively. For conjunctive and disjunctive operators, we define the weights as $w := [w_i]_{i=1:N} \in \mathbb{R}_{>0}^N$, where N is the number of subformulae in the operator. For temporal operators, we define the weights as $w := [w_k]_{k \in I} \in \mathbb{R}_{>0}^{|I|}$ for interval I . For notational simplicity, we use the following notation interchangeably: $\bigwedge_{i=1}^N w\phi_i = \bigwedge_{i=1}^N w_i\phi_i$ and $\bigvee_{i=1}^N w\phi_i = \bigvee_{i=1}^N w_i\phi_i$.

B. Normalized wSTL

Our neural network architecture proposed in Section III-A requires the weights within each operator to be normalized. We discuss the reasons for this requirement in Section III-E. Given this requirement, we define normalized wSTL syntax recursively as $\phi := \top \mid \psi \mid \neg\phi \mid \bigwedge_{i=1}^N w\phi_i \mid \bigvee_{i=1}^N w\phi_i \mid \mathcal{G}_I^w\phi \mid \mathcal{F}_I^w\phi$, where all terminology carries over from wSTL, except we further require $\sum_{i=1}^N w_i = \sum_{k \in I} w_k = 1$, where $w_i, w_k \in [0, 1]$. We allow the weights to be zero because the zero weights do not influence the overall robustness [21].

To avoid large input values to our neural network, we also define normalized quantitative satisfaction semantics, or *robustness*, by extending [20] as follows,

$$r(\psi, \tau, t) := \begin{cases} \frac{f(s_t) - c}{\sup_{s \in S} f(s) - c} & \text{if } f(s_t) - c \geq 0, \\ \frac{f(s_t) - c}{\inf_{s \in S} f(s) - c} & \text{otherwise} \end{cases}, \quad (1)$$

$$r(\neg\phi, \tau, t) := -r(\phi, \tau, t), \quad (2)$$

$$r\left(\bigwedge_{i=1}^N w\phi_i, \tau, t\right) := \otimes^\wedge(w, [r(\phi_i, \tau, t)]_{i=1:N}), \quad (3)$$

$$r\left(\bigvee_{i=1}^N w\phi_i, \tau, t\right) := \oplus^\vee(w, [r(\phi_i, \tau, t)]_{i=1:N}), \quad (4)$$

$$r(\mathcal{G}_I^w\phi, \tau, t) := \otimes^\mathcal{G}(w, [r(\phi, \tau, t')]_{t' \in t+I}), \quad (5)$$

$$r(\mathcal{F}_I^w\phi, \tau, t) := \oplus^\mathcal{F}(w, [r(\phi, \tau, t')]_{t' \in t+I}), \quad (6)$$

where the aggregation functions $\otimes^\wedge : \mathbb{R}_{>0}^N \times \mathbb{R}^N \rightarrow \mathbb{R}$, $\otimes^\vee : \mathbb{R}_{>0}^N \times \mathbb{R}^N \rightarrow \mathbb{R}$, $\otimes^\mathcal{G} : \mathbb{R}_{>0}^{|I|} \times \mathbb{R}^{|I|} \rightarrow \mathbb{R}$, and $\otimes^\mathcal{F} : \mathbb{R}_{>0}^{|I|} \times \mathbb{R}^{|I|} \rightarrow \mathbb{R}$ correspond to the operators \wedge , \vee , \mathcal{G} , and \mathcal{F} , respectively. For notational simplicity, we interchangeably use $r(\phi, \tau, t)$ and $r_{\tau t}^\phi$.

Building from [21], we define the aggregation functions with a scaling constant $\sigma > 0$ as follows,

$$\otimes^\wedge(w, [r_{\tau t}^{\phi_i}]_{i=1:N}) := \frac{\sum_{i=1}^N w_i r_{\tau t}^{\phi_i} \exp(\frac{-r_{\tau t}^{\phi_i}}{\sigma})}{\sum_{i=1}^N w_i \exp(\frac{-r_{\tau t}^{\phi_i}}{\sigma})}, \quad (7)$$

$$\oplus^\vee(w, [r_{\tau t}^{\phi_i}]_{i=1:N}) := \frac{\sum_{i=1}^N w_i r_{\tau t}^{\phi_i} \exp(\frac{r_{\tau t}^{\phi_i}}{\sigma})}{\sum_{i=1}^N w_i \exp(\frac{r_{\tau t}^{\phi_i}}{\sigma})}, \quad (8)$$

$$\otimes^\mathcal{G}(w, [r_{\tau t'}^\phi]_{t' \in t+I}) := \frac{\sum_{t' \in t+I} w_{t'} r_{\tau t'}^\phi \exp(\frac{-r_{\tau t'}^\phi}{\sigma})}{\sum_{t' \in t+I} w_{t'} \exp(\frac{-r_{\tau t'}^\phi}{\sigma})}, \quad (9)$$

$$\oplus^\mathcal{F}(w, [r_{\tau t'}^\phi]_{t' \in t+I}) := \frac{\sum_{t' \in t+I} w_{t'} r_{\tau t'}^\phi \exp(\frac{r_{\tau t'}^\phi}{\sigma})}{\sum_{t' \in t+I} w_{t'} \exp(\frac{r_{\tau t'}^\phi}{\sigma})}. \quad (10)$$

We use $\sigma = 0.5$ in this work.

C. Problem Statement

We consider the following binary classification task. Let $\mathcal{T} = \{(\tau_i, l_i)\}_{i=1:N_{\text{data}}}$ be a labeled dataset, where $\tau_i \in \mathbb{R}^{n \times H}$ is the i^{th} trajectory with label $l_i \in \{1, -1\}$ and $N_{\text{data}} \in \mathbb{Z}_{>0}$ is the number of data points in the dataset.

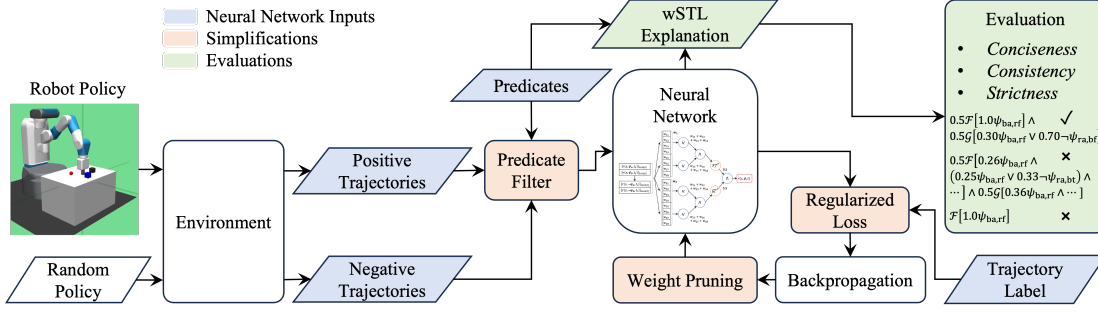


Fig. 2. We propose a neuro-symbolic approach for generating an explanation of a given robot policy using wSTL. Our network architecture, TLNET, includes a simplification process that ensures resulting explanations balance classification accuracy with conciseness, consistency, and strictness.

Problem 1. Given a dataset \mathcal{T} , find a wSTL specification ϕ that balances classification accuracy with conciseness, consistency, and strictness.

III. METHODOLOGY

We first introduce our neural network architecture, TLNET, which allows us to represent wSTL structures in a fully differentiable form. We then introduce our simplification process, which enhances the explainability of inferred explanations, and our trajectory sampling process. Finally, we propose novel evaluation metrics for explainability—*conciseness*, *consistency*, and *strictness*—and provide theoretical justification for our network architecture. Figure 2 and Algorithm 1 summarize our overall approach.

A. Neural Network Architecture

Let $\Psi = \{\psi_i\}_{i=1:N_{AP}}$ be a predefined set of atomic predicates and $\Psi_- = \{\neg\psi_i\}_{i=1:N_{AP}}$ be a set of their negations. We focus on representing normalized wSTL structures composed of temporal operators containing these predicates in conjunctive normal form (CNF), as follows,

$$\phi = 0.5\mathcal{F}_I^{\bar{w}} \left[\bigwedge_{i=1}^{N_{AP}} w_i^{\mathcal{F}} \bigvee_{j=1}^{2N_{AP}} w_{ij}^{\mathcal{F}} \psi_j \right] \wedge 0.5\mathcal{G}_I^{\bar{w}} \left[\bigwedge_{i=1}^{N_{AP}} w_i^{\mathcal{G}} \bigvee_{j=1}^{2N_{AP}} w_{ij}^{\mathcal{G}} \psi_j \right], \quad (11)$$

where $w_i^{\mathcal{F}}, w_{ij}^{\mathcal{F}}, w_i^{\mathcal{G}}, w_{ij}^{\mathcal{G}} \in [0, 1]$ are importance weights and $\psi_j \in \Psi \cup \Psi_-$ are predefined atomic predicates. We define the weights \bar{w} for temporal operators over interval $I = [0, H]$ to be $\bar{w} = [\bar{w}_k = 1/|I|]_{k=1:|I|}$ for trajectory τ . We define the conjunction weights of the temporal clauses to be 0.5 to equally weigh the importance of the task (\mathcal{F}) and constraint (\mathcal{G}) parts of the explanation. We choose this class of structures because they allow us to represent a general class of robot policies aiming to complete a task while satisfying a set of constraints [19], [26].

We represent specifications of the form given in Equation (11) by designing a neural network f_w parameterized by w , where w defines the importance weights of the currently represented specification ϕ_w . The input to the neural network

Algorithm 1 Explanation Generation

Input: Dataset \mathcal{T} , predicates $\Psi = \{\psi_i\}_{i=1:N_{AP}}$, similarity threshold S_{th} , number of pruning iterations N_{pr} , number of weights to prune N_w , loss function $\tilde{\mathcal{L}}$.

Output: Explanation ϕ

- 1: Evaluate robustness of trajectories in \mathcal{T} using Ψ .
- 2: Filter out predicates whose similarities are above S_{th} .
- 3: Initialize the neural network f_w with parameters w .
- 4: Optimize w to minimize $\tilde{\mathcal{L}}$.
- 5: **for** $i = 1 : N_{pr}$ **do**
- 6: Prune zeroed and smallest N_w parameters in w .
- 7: Re-normalize w .
- 8: Optimize w to minimize $\tilde{\mathcal{L}}$.
- 9: **if** only one non-zero weight in $w^{\mathcal{F}}/w^{\mathcal{G}}$ **then break**.
- 10: **return** ϕ generated from w and Ψ using Equation (12).

is a sequence of the robustness values for each predicate $\psi \in \Psi \cup \Psi_-$ for each timestep in a trajectory τ . The output is the robustness of the current specification, $r(\phi_w, \tau)$, for that trajectory. The neural network is trained to minimize a regularized classification loss (discussed in Section III-B), given a labeled dataset \mathcal{T} .

We reduce the number of parameters that are optimized by distributing the weights in Equation (11), resulting in a specification of the following form,

$$\phi_w = 0.5\mathcal{F}_I^{\bar{w}} \left[\bigwedge_{i=1}^{N_{AP}} \bigvee_{j=1}^{2N_{AP}} \tilde{w}_{ij}^{\mathcal{F}} \psi_j \right] \wedge 0.5\mathcal{G}_I^{\bar{w}} \left[\bigwedge_{i=1}^{N_{AP}} \bigvee_{j=1}^{2N_{AP}} \tilde{w}_{ij}^{\mathcal{G}} \psi_j \right], \quad (12)$$

where $w = w^{\mathcal{F}} \parallel w^{\mathcal{G}}$, $w^{\mathcal{F}} = [\tilde{w}_{ij}^{\mathcal{F}}]_{i=1:N_{AP}, j=1:2N_{AP}}$, $w^{\mathcal{G}} = [\tilde{w}_{ij}^{\mathcal{G}}]_{i=1:N_{AP}, j=1:2N_{AP}}$, $\tilde{w}_{ij}^{\mathcal{F}} = w_i^{\mathcal{F}} w_{ij}^{\mathcal{F}}$, and $\tilde{w}_{ij}^{\mathcal{G}} = w_i^{\mathcal{G}} w_{ij}^{\mathcal{G}}$. We justify this weight distribution operation in Section III-E. An example TLNET architecture for a dataset containing two predicates is shown in Figure 3.

B. Simplification Process

A key component of TLNET is its simplification process, which aims to produce more human-interpretable wSTL explanations while preserving classification performance.

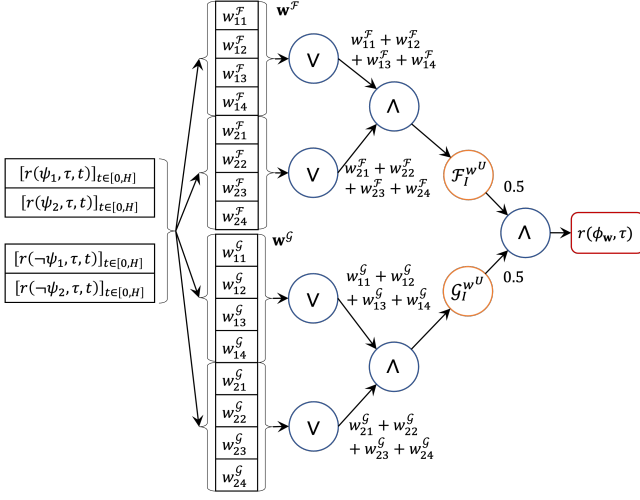


Fig. 3. Example architecture of the proposed neural network when there are two predicates to consider (ψ_1 and ψ_2). \mathbf{w}^F and \mathbf{w}^G are weight vectors that are optimized. ϕ is the inferred explanation to the given trajectory.

This process consists of three steps: a predicate filter, loss regularization, and weight pruning.

1) *Predicate Filter*: As a pre-processing step, we implement a predicate filter that eliminates predicates that exhibit similar behavior across both positive and negative trajectory sets, as they contribute little to discriminating between those sets and may introduce unnecessary complexity. Given an arbitrary dataset of trajectories \mathcal{D} and an atomic predicate ψ , we define the *robustness distribution* for ψ as,

$$d(\mathcal{D}, \psi) = \frac{1}{|\mathcal{D}|} [|\mathcal{D}_1|, |\mathcal{D}_2|, |\mathcal{D}_3|], \quad (13)$$

$$\mathcal{D}_1 := \{ \tau \mid r(\psi, \tau, t) \geq 0 \quad \forall t \in [0, H], \tau \in \mathcal{D} \}, \quad (14)$$

$$\mathcal{D}_2 := \mathcal{D} \setminus (\mathcal{D}_1 \cup \mathcal{D}_3), \quad (15)$$

$$\mathcal{D}_3 := \{ \tau \mid r(\psi, \tau, t) < 0 \quad \forall t \in [0, H], \tau \in \mathcal{D} \}. \quad (16)$$

That is, \mathcal{D}_1 is the set of trajectories where ψ is always satisfied, \mathcal{D}_2 is the set where ψ is satisfied at least once, and \mathcal{D}_3 is the set where ψ is never satisfied.

Now, let $\mathcal{T}_p = \{(\tau, l) \mid l = 1, (\tau, l) \in \mathcal{T}\}$ be the positive set of trajectories in \mathcal{T} and $\mathcal{T}_n = \mathcal{T} \setminus \mathcal{T}_p$ be the negative set. For each predicate $\psi \in \Psi$, we then calculate $d(\mathcal{T}_p, \psi)$ and $d(\mathcal{T}_n, \psi)$, and then calculate the cosine similarity S between those distributions. We then remove predicates from the set Ψ (and their negation from Ψ_-) which have a cosine similarity $S > S_{th}$, where S_{th} is a user-defined threshold.

2) *Loss Regularization*: The regularization step uses two regularizers to improve the conciseness of inferred explanations. The first regularizer, a *temporal clause regularizer*, R_T , is defined as,

$$R_T(\mathbf{w}) := \sum_{j=1}^{N_{AP}} \max \left(\sum_{i=1}^{N_{AP}} \tilde{w}_{ij}^F, \sum_{i=1}^{N_{AP}} \tilde{w}_{i(j+N_{AP})}^F \right) \max \left(\sum_{i=1}^{N_{AP}} \tilde{w}_{ij}^G, \sum_{i=1}^{N_{AP}} \tilde{w}_{i(j+N_{AP})}^G \right). \quad (17)$$

Intuitively, this regularizer encourages the task and constraint clauses to contain different atomic predicates.

The second regularizer, a *disjunctive clause regularizer*, R_D , is defined as,

$$R_D(\mathbf{w}^O) := \sum_{i=1}^{N_{AP}-1} \sum_{j=i+1}^{N_{AP}} \sum_{k=1}^{2N_{AP}} \tilde{w}_{ik}^O \tilde{w}_{jk}^O, \quad (18)$$

where $\mathbf{w}^O \in \{\mathbf{w}^F, \mathbf{w}^G\}$ defines the weights within one of our temporal operators and $\tilde{w}_{ij}^O, \tilde{w}_{jk}^O \in \mathbf{w}^O$. Intuitively, this regularizer encourages disjunctive clauses within a temporal clause to contain different predicates.

Given $(\tau, l) \in \mathcal{T}$, our overall loss, $\tilde{\mathcal{L}}$, is then,

$$\tilde{\mathcal{L}}(\tau, l, \mathbf{w}) = \mathcal{L}(\tau, l, \mathbf{w}) + \lambda_{R_T} R_T(\mathbf{w}) + \lambda_{R_D} [R_D(\mathbf{w}^F) + R_D(\mathbf{w}^G)], \quad (19)$$

where \mathcal{L} is a classification loss and $\lambda_{R_T}, \lambda_{R_D} \in \mathbb{R}_{\geq 0}$ are regularizer hyperparameters. We use $\lambda_{R_T} = 0.01$ and $\lambda_{R_D} = 0.1$ for this work. We use the classification loss from [21],

$$\mathcal{L}(\tau, l, \mathbf{w}) = \exp(-\zeta \ln(r(\phi_{\mathbf{w}}, \tau))), \quad (20)$$

where $\zeta \in \mathbb{R}_{>0}$ is a hyperparameter ($\zeta = 1$ for this work).

3) *Weight Pruning*: The weight pruning step further simplifies the currently inferred explanation by removing unnecessary weights. First, all weights with a value of zero are removed from the network. Then, among the remaining weights, the $N_w \in \mathbb{Z}_{>0}$ smallest weights—where N_w is a user-specified hyperparameter—are removed to eliminate the least contributing parts of the specification. The remaining weights are then normalized. The pruning process terminates if there is only one non-zero weight in \mathbf{w}^F or \mathbf{w}^G to ensure the task-constraint structure of the inferred explanation.

C. Trajectory Sampling

We obtain positive trajectories in \mathcal{T} by executing the target policy in the environment. These trajectories can also be sampled from existing datasets. We obtain negative trajectories in \mathcal{T} by executing a random-walk policy in the environment.

D. Explainability Evaluation Metrics

Beyond classification performance, TLNET also emphasizes the human-interpretability of inferred explanations. We quantify this emphasis by introducing three explainability metrics—*conciseness*, *consistency*, and *strictness*.

Let ϕ be a wSTL explanation we want to evaluate and N be the number of temporal clauses that we expect to appear in the explanation. For example, in this work, we expect the inferred explanations to have one \mathcal{F} clause and one \mathcal{G} clause (thus $N = 2$) because we assume there should be a task component and a constraint component. Now, let ϕ_n be the n -th expected temporal clause in ϕ , where $\phi_n = \emptyset$ if that clause does not exist in ϕ . Let the (unweighted) STL counterpart of ϕ_n be $\hat{\phi}_n$, where $n \in \{1, \dots, N\}$. For example, in our work, if $\phi = \mathcal{G}(0.1\psi_1 \wedge 0.9\psi_2)$, then $\phi_1 = \emptyset$, $\hat{\phi}_1 = \emptyset$, $\phi_2 = \mathcal{G}(0.1\psi_1 \wedge 0.9\psi_2)$, and $\hat{\phi}_2 = \mathcal{G}(\psi_1 \wedge \psi_2)$.

1) *Conciseness*: We define the *conciseness* of ϕ as,

$$\text{Conciseness} := \frac{1}{N} \sum_{n=1}^N \begin{cases} \frac{1}{m_n} & \text{if } m_n \neq 0, \\ 0 & \text{otherwise,} \end{cases}$$

where m_n is the number of predicates present in n -th expected temporal clause ϕ_n . Conciseness ranges from 0 to 1, with higher scores implying a shorter explanation with at least one predicate inside each expected temporal clause.

2) *Consistency*: Let $\Phi = [\phi^k]_{k=1:K}$ be a sequence of K explanations for the same policy (e.g., from different training seeds). Then, let $\Phi_n = [\phi_n^k]_{k=1:K}$ be the sequence of the n -th expected temporal clauses in Φ , where ϕ_n^k is the n -th expected temporal clause for ϕ^k . Let the STL counterpart of Φ_n be $\hat{\Phi}_n$. Then, let the set of unique elements of $\hat{\Phi}_n$ be $\Sigma_n = \{\hat{\phi}_n \in \hat{\Phi}_n\}$. We define the *consistency* of Φ as,

Consistency :=

$$\frac{1}{N} \sum_{n=1}^N \begin{cases} \max_{\sigma_n \in \Sigma_n} \sum_{\hat{\phi}_n \in \hat{\Phi}_n} \frac{\mathbf{1}_{\sigma_n}(\hat{\phi}_n)}{K|\Sigma_n|} & \text{if } \Sigma_n \neq \emptyset, \\ 0 & \text{otherwise,} \end{cases}$$

where $\mathbf{1}_{\sigma_n}(\cdot)$ is the indicator function for σ_n . Consistency ranges from 0 to 1, with higher scores indicating greater agreement in clause structures across explanations, reflecting structural stability in learned explanations.

3) *Strictness*: Finally, let P be the number of potentially present predicates in ϕ (e.g., $P = 2N_{\text{AP}}$ in TLNET). Denote the numbers of conjunctions and disjunctions in ϕ_n as C_n and D_n , respectively. We define the *strictness* of ϕ as,

$$\text{Strictness} := \frac{1}{N} \sum_{n=1}^N \begin{cases} \frac{1}{P - C_n + D_n} & \text{if } \phi_n \neq \emptyset, \\ 0 & \text{otherwise.} \end{cases}$$

Strictness ranges from 0 to 1, with higher scores implying stricter logical expressions by rewarding conjunctions and penalizing disjunctions.

E. Weight Distribution in wSTL

A key assumption in TLNET is that the weights can be distributed across Boolean and temporal clauses. We now prove that such a distribution is theoretically sound. The normalized weights of a wSTL formula in CNF can be syntactically distributed across Boolean operators as follows.

Theorem 1 (Syntactic Weight Distributivity of Boolean Operators). A normalized wSTL formula ϕ in CNF can be represented as follows,

$$\phi = \bigwedge_{i=1}^n w_i \bigvee_{j=1}^{m_i} w_{ij}(\neg) \psi_{ij} \equiv \bigwedge_{i=1}^n \bigvee_{j=1}^{m_i} \tilde{w}_{ij}(\neg) \psi_{ij}, \quad (21)$$

where $n, m_i \in \mathbb{Z}_{>0}$, $w_i, w_{ij} \in \mathbb{R}_{>0}$, $\tilde{w}_{ij} := w_i w_{ij}$, $\sum_{i=1}^n w_i = \sum_{j=1}^{m_i} w_{ij} = 1$, and ψ_{ij} are predicates. Furthermore, the weights \tilde{w}_{ij} satisfy $\sum_{i=1}^n \sum_{j=1}^{m_i} \tilde{w}_{ij} = 1$.

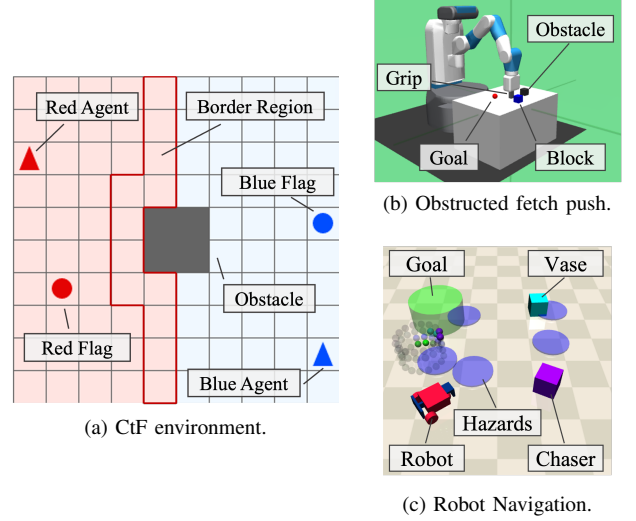


Fig. 4. Screenshots from our environments.

Proof.

$$\begin{aligned} \{\text{LHS}\} &= w_1(w_{11}(\neg)\psi_{11} \vee \dots \vee w_{1m_1}(\neg)\psi_{1m_1}) \\ &\quad \dots \wedge w_n(w_{n1}(\neg)\psi_{n1} \vee \dots \vee w_{nm_n}(\neg)\psi_{nm_n}) \\ &= (w_1w_{11}(\neg)\psi_{11} \vee \dots \vee w_1w_{1m_1}(\neg)\psi_{1m_1}) \\ &\quad \dots \wedge (w_nw_{n1}(\neg)\psi_{n1} \vee \dots \vee w_nw_{nm_n}(\neg)\psi_{nm_n}) \\ &= \bigwedge_{i=1}^n \bigvee_{j=1}^{m_i} w_iw_{ij}(\neg)\psi_{ij} = \{\text{RHS}\}. \end{aligned}$$

□

IV. RESULTS

We perform a series of empirical experiments to compare our method to relevant baselines for robotic tasks. We consider three baselines for inference of wSTL explanations, each adapted to model our normalized wSTL structures (given by Equation (12)):

- *NN-TLI* [25]: this method implements a greedy pruning strategy that independently removes network weights that do not affect classification accuracy after optimization. We removed their weight-rounding process (to convert to STL) to consider the structure in Equation (12) and used the aggregation functions given in Section II-B, since our empirical results showed more training stability with those functions.
- *STONE (top-3)* [21]: this method retains the 3 largest network weights after training.
- *STONE (top-5)* [21], [24]: this method retains the 5 largest network weights after training.

All baselines were implemented using the same neural network architecture as TLNET to ensure a consistent basis for comparison. For each policy we explain, we collected 500 positive trajectories using the trained policy and 500 negative trajectories using a random-walk policy. Each dataset was split 80% and 20% for training and evaluation, respectively. Our code is available on GitHub after acceptance.

A. Test Environments

We consider the three environments shown in Figure 4, which include discrete and continuous state-action spaces, navigation and manipulation tasks, and varied predicates.

1) *Capture-the-flag (CtF)*: CtF is a discrete grid-world environment with adversarial dynamics where two agents compete to capture each other’s flags, based on [19]. If both agents occupy adjacent cells in a given territory, the defending agent eliminates the other with 75% probability. We considered blue agent policies optimized for five scenarios. The first four considered different red agent heuristic policies (*capture*, *fight*, *patrol*, *mixture*) with the same reward function (capture: +1, kill: +0.5, being captured: −1, timestep penalty: −0.01). The fifth scenario (*capture 0*) used a capture red agent with the reward function modified to remove the kill reward (kill: 0). The red agent policies are defined as follows: *capture* pursues the flag; *fight* pursues the blue agent; *patrol* defends a boundary region; and *mixture* switches between capturing and defending. Red agents perform a random action 25% of the time. We defined eight atomic predicates based on the defeated (“df”) status $\{1, -1\}$ of the red agent and euclidean distances among the blue agent (“ba”), blue flag (“bf”), blue territory (“bt”), red agent (“ra”), red flag (“rf”), and obstacle (“ob”): $\psi_{ba,bt}$, $\psi_{ba,ob}$, $\psi_{ba,ra}$, $\psi_{ba,rf}$, $\psi_{ra,bf}$, $\psi_{ra,bt}$, $\psi_{ra,df}$, $\psi_{ra,ob}$.

2) *Fetch Push*: We also consider a continuous control task based on the Fetch mobile manipulator [27]. The robot must push a blue block (“b”) to a red target (“t”) using its gripper (“g”), without disturbing a black obstacle (“o”). The state and action spaces are continuous ($s \in \mathbb{R}^{55}$, $a \in \mathbb{R}^4$). Eight predicates were defined based on the distances between the gripper, block, target, and obstacle, including drop-related (“d”) conditions: ψ_{gb} , ψ_{gt} , ψ_{go} , ψ_{bt} , ψ_{bo} , ψ_{ot} , ψ_{bd} , ψ_{od} .

3) *Robot Navigation*: Finally, we extended the CarGoal-v0 environment [28] to create a more complex adversarial navigation task. The ego robot (“e”) must reach a green goal (“g”) while avoiding a violet chaser (“c”) moving with a fixed speed ($v_c = 7.5 \times 10^{-4}$). Static hazards (“h”) and a movable vase (“v”) are present but not penalized. The state and action dimensions are $s \in \mathbb{R}^{88}$ and $a \in \mathbb{R}^2$, respectively. Ten distance-based predicates were defined, involving euclidean distances between the robot, the chaser, the goal, and the hazards: ψ_{ec} , ψ_{eg} , ψ_{eh} , ψ_{ev} , ψ_{gc} , ψ_{gh} , ψ_{gv} , ψ_{hc} , ψ_{hv} , ψ_{vc} .

We included predicates irrelevant to task success in each environment (e.g., $\psi_{ra,ob}$, ψ_{ot} , ψ_{hv}) to evaluate whether the considered methods could eliminate them from their explanations.

B. Policy Optimization

TLNET is a general framework to generate explanations of robot policies, though, we focused on policies optimized by deep reinforcement learning algorithms in this work. We used Stable-Baselines3 [29] for training all policies. For the CtF and navigation environments, PPO [30] was used; for the Fetch Push task, we used SAC [31] with hindsight experience replay (HER) [32]. Hyperparameters were taken from prior work [19], [28], [33]. For each policy, we performed 10

independent optimization runs with random initialization and collected classification accuracy and explainability metrics. The time horizon (H) for each environment is 100 for CtF, 200 for Fetch Push, and 400 for Robot Navigation.

C. Experimental Results

1) *Benefits and Limitations of TLNET*: Table I presents the most frequent explanation obtained by each method for each scenario. Across all scenarios, TLNET consistently inferred both task and constraint clauses, while also producing concise and relatively easy-to-understand explanations. In comparison, NN-TLI typically yielded verbose explanations that are difficult to understand, while STONE often captured only one temporal clause, resulting in incomplete explanations.

The explanations produced by TLNET are also qualitatively reasonable (and often correct). For example, for all CtF scenarios, TLNET correctly inferred the task clause as $\psi_{ba,rf}$ (“blue agent captures the red flag”)—no other method correctly inferred this task for every scenario. The inferred CtF constraints are also syntactically reasonable. For example, in the Capture scenario, the blue agent (global) constraint includes “red agent not on the blue flag” because the capture red policy only targets the blue flag, which required the blue agent to learn to prevent the red agent from reaching the blue flag. Other scenarios, such as Fight and Patrol, did not include this predicate in the inferred constraint because those red policies do not target the blue flag. In comparison, the CtF constraints inferred by NN-TLI are generally too verbose to understand, while STONE did not infer any constraints.

For Fetch Push, TLNET also correctly inferred the task clause as ψ_{bt} (“block reaches the target”), which no other method correctly inferred. While TLNET inferred part of the expected constraint (ψ_{gb}, ψ_{bt}), it missed an expected constraint $\neg\psi_{go}$ (“grip does not touch the obstacle”), likely due to insufficient occurrences of the grip touching the obstacle in the sampled data. Future research could mitigate this issue by introducing more intelligent sampling strategies for generating the negative dataset (e.g., adversarial or targeted trajectory sampling). NN-TLI also inferred part of the expected constraint, but also missed the $\neg\psi_{go}$ constraint. Meanwhile, both variations of STONE inferred an incorrect constraint of ψ_{bt} (“block reaches the target”), since this is actually the task and not possible to always satisfy.

For Robot Navigation, all methods correctly inferred the task clause but TLNET was the only one to infer the correct constraint clause as $\neg\psi_{ec}$ (“the robot does not hit the chaser”).

As shown in Table II, TLNET also outperformed all baselines in conciseness, consistency, and strictness, with marginal differences in classification accuracy. Across all scenarios, TLNET achieved up to $1.9\times$ higher conciseness, $2.6\times$ higher consistency, and $2.7\times$ higher strictness. These results support the qualitative findings above, validating the explainability of our method’s outputs and the use of these explainability metrics.

TABLE I
COMPARISON OF THE MOST FREQUENTLY INFERRED EXPLANATIONS.

Scenarios	TLNET (Ours)	NN-TLI	STONE (top-3)	STONE (top-5)
CtF Capture	$0.5\mathcal{F}_I^w[1.0\psi_{ba,rf}] \wedge$ $0.5\mathcal{G}_I^w[0.30\psi_{ba,rf} \vee 0.70\neg\psi_{ra,bf}]$	$0.5\mathcal{F}_I^w[0.26\psi_{ba,rf} \wedge (0.25\psi_{ba,rf} \vee 0.33\neg\psi_{ra,bt}) \wedge$ $(0.09\neg\psi_{ba,bt} \vee 0.07\neg\psi_{ra,bt})] \wedge$ $0.5\mathcal{G}_I^w[0.36\psi_{ba,rf} \vee 0.64\neg\psi_{ra,bf}]$	$\mathcal{F}_I^w[0.73\neg\psi_{ra,bt}$ $\wedge 0.27\neg\psi_{ba,bt}]$	$\mathcal{F}_I^w[0.83\neg\psi_{ra,bt}$ $\wedge 0.17\psi_{ba,rf}]$
CtF Fight	$0.5\mathcal{F}_I^w[1.0\psi_{ba,rf}] \wedge$ $0.5\mathcal{G}_I^w[0.33\psi_{ba,rf} \vee 0.67\neg\psi_{ba,ra}]$	$0.5\mathcal{F}_I^w[0.77\psi_{ba,rf} \wedge (0.15\psi_{ba,rf} \vee 0.08\psi_{ra,bf})] \wedge$ $0.5\mathcal{G}_I^w[(0.15\neg\psi_{ba,bt} \vee 0.11\neg\psi_{ra,df}) \wedge 0.06\psi_{ba,rf}$ $\vee 0.04\neg\psi_{ra,df}) \wedge (0.06\psi_{ba,rf} \vee 0.06\neg\psi_{ba,bt} \vee$ $0.04\neg\psi_{ra,df}) \wedge (0.02\psi_{ba,ra} \vee 0.19\psi_{ba,rf} \vee$ $0.16\neg\psi_{ba,bt} \vee 0.11\neg\psi_{ra,df})]$	$\mathcal{F}_I^w[1.0\psi_{ba,rf}]$	$\mathcal{F}_I^w[1.0\psi_{ba,rf}]$
CtF Patrol	$0.5\mathcal{F}_I^w[1.0\psi_{ba,rf}] \wedge$ $0.5\mathcal{G}_I^w[0.52\psi_{ba,rf} \vee 0.48\neg\psi_{ra,bt}]$	$0.5\mathcal{F}_I^w[0.35\psi_{ba,rf} \wedge (0.09\psi_{ba,rf} \vee 0.55\psi_{ra,df})] \wedge$ $0.5\mathcal{G}_I^w[(0.29\psi_{ba,rf} \vee 0.04\psi_{ra,bf} \vee 0.07\neg\psi_{ra,df}) \wedge$ $(0.30\psi_{ba,rf} \vee 0.19\psi_{ra,bf} \vee 0.02\neg\psi_{ba,bt}) \wedge$ $0.04\psi_{ra,bf} \wedge 0.05\neg\psi_{ra,bf}]$	$\mathcal{F}_I^w[1.0\psi_{ra,df}]$	$\mathcal{F}_I^w[1.0\psi_{ra,df}]$
CtF Mixture	$0.5\mathcal{F}_I^w[1.0\psi_{ba,rf}] \wedge$ $0.5\mathcal{G}_I^w[0.44\psi_{ba,rf} \vee 0.56\neg\psi_{ra,bf}]$	$0.5\mathcal{F}_I^w[1.0\psi_{ba,rf}] \wedge 0.5\mathcal{G}_I^w[0.21\neg\psi_{ra,bf} \wedge 0.47\psi_{ba,rf}$ $\wedge (0.04\neg\psi_{ra,bf} \vee 0.05\neg\psi_{ra,df}) \wedge (0.18\psi_{ba,rf} \vee$ $0.03\psi_{ra,df} \vee 0.04\neg\psi_{ra,bf} \vee 0.02\neg\psi_{ra,bt})]$	$\mathcal{F}_I^w[1.0\psi_{ba,bt}]$	$\mathcal{F}_I^w[0.48\neg\psi_{ba,bt}$ $\wedge 0.52\psi_{ba,rf}]$
CtF Capture 0	$0.5\mathcal{F}_I^w[1.0\psi_{ba,rf}] \wedge$ $0.5\mathcal{G}_I^w[0.31\psi_{ba,rf} \vee 0.69\neg\psi_{ra,bf}]$	$0.5\mathcal{F}_I^w[0.08\psi_{ba,rf} \wedge (0.40\psi_{ba,rf} \vee 0.31\neg\psi_{ra,bt}) \wedge$ $(0.07\neg\psi_{ba,bt} \vee 0.14\neg\psi_{ra,bt})] \wedge 0.5\mathcal{G}_I^w[(0.33\psi_{ba,rf}$ $\vee 0.58\neg\psi_{ra,bf}) \wedge (0.05\psi_{ba,rf} \vee 0.04\neg\psi_{ra,bt})]$	$\mathcal{F}_I^w[0.67\neg\psi_{ra,bt}$ $\wedge 0.33\neg\psi_{ba,bt}]$	$\mathcal{F}_I^w[0.83\neg\psi_{ra,bt}$ $\wedge 0.17\psi_{ba,rf}]$
Fetch Push	$0.5\mathcal{F}_I^w[1.0\psi_{bt}] \wedge$ $0.5\mathcal{G}_I^w[0.41\psi_{gb} \vee 0.59\psi_{bt}]$	$0.5\mathcal{F}_I^w[0.74\psi_{bt} \wedge (0.10\psi_{bt} \vee 0.16\psi_{od})] \wedge$ $0.5\mathcal{G}_I^w[1.0\neg\psi_{bd}]$	$\mathcal{G}_I^w[1.0\psi_{bt}]$	$\mathcal{G}_I^w[1.0\psi_{bt}]$
Robot Navi.	$0.5\mathcal{F}_I^w[1.0\psi_{eg}] \wedge 0.5\mathcal{G}_I^w[1.0\neg\psi_{ec}]$	$\mathcal{F}_I^w[1.0\psi_{eg}]$	$\mathcal{F}_I^w[1.0\psi_{eg}]$	$\mathcal{F}_I^w[1.0\psi_{eg}]$

TABLE II
COMPARISON OF CONCISENESS, CONSISTENCY, STRICTNESS, AND ACCURACY METRICS. THE BEST RESULTS ARE BOLD.

Scenarios	Conciseness				Consistency				Strictness				Accuracy			
	Ours	NN-TLI	STONE		Ours	NN-TLI	STONE		Ours	NN-TLI	STONE		Ours	NN-TLI	STONE	
CtF Capture	0.41	0.21	0.20	0.22	0.33	0.08	0.08	0.13	0.33	0.08	0.08	0.13	0.95	0.95	0.95	0.94
CtF Fight	0.39	0.18	0.25	0.25	0.68	0.09	0.50	0.50	0.68	0.09	0.50	0.50	0.94	0.92	0.94	0.93
CtF Patrol	0.38	0.18	0.25	0.28	0.63	0.05	0.50	0.53	0.63	0.05	0.50	0.53	0.95	0.93	0.94	0.94
CtF Mixture	0.39	0.12	0.21	0.16	0.27	0.06	0.10	0.09	0.27	0.06	0.10	0.09	0.87	0.89	0.88	0.88
CtF Capt. 0	0.42	0.21	0.20	0.30	0.45	0.11	0.15	0.24	0.45	0.11	0.15	0.24	0.95	0.95	0.95	0.95
Fetch Push	0.42	0.31	0.25	0.25	1.00	0.28	0.50	0.50	1.00	0.28	0.50	0.50	0.99	0.97	0.97	0.97
Robot Navi.	0.48	0.22	0.25	0.25	0.68	0.15	0.50	0.50	0.68	0.15	0.50	0.50	0.97	0.96	0.96	0.96

2) *Benefit of Including Weights:* We now demonstrate the benefit of including weights within inferred explanations (e.g., using wSTL rather than STL [25] or LTL [16]–[18]) by examining how inferred weights differ across CtF scenarios. Consider the Capture and Mixture explanations in Table I. Both capture and mixture red policies target the blue flag, but the capture policy is more aggressive in doing so. The blue agent, in response, learns slightly different policies: a more defensive policy in Capture, prioritizing the protection of its flag, and a more aggressive policy in Mixture, focusing more on capturing the red flag. This policy difference is reflected in the weights in the constraint clause, where the $\neg\psi_{ra,bf}$ predicate receives a higher weight in the Capture explanation (0.70) than in the Mixture explanation (0.56), due to the Capture policy’s prioritization of flag protection. Conversely, the Mixture policy shows a higher weight for the $\psi_{ba,rf}$ predicate (0.44) than the Capture policy (0.30), due to the Mixture policy’s prioritization of flag capture. Note that $\psi_{ba,rf}$ appears in both the task and constraint clauses in these explanations. This duplication results from our design choice to fix equal weights (0.5) on the task and constraint clauses, which forces TLNET to express prioritization between the task and constraint by including relevant task predicates in the constraint clause. Although one could alternatively

include the task and constraints weights within the optimized parameters, we found that doing so introduced training instability.

Now, consider the Capture and Capture 0 scenarios, which differ in the reward to kill the red agent (0.5 vs. 0). While one might naively expect this difference to produce different policy explanations, it actually should not change the optimal blue agent policies because, to win the game, the blue agent should first defend its flag (by killing the red agent), since the red agent uses the capture policy. We see that TLNET successfully captured this nuance by inferring constraints with nearly identical weights, reflecting its robustness to minor reward differences that still lead to similar policies. NN-TLI and STONE did not infer similar constraints across these scenarios. More broadly, this result also demonstrates the importance of inferring explanations from actual observed behaviors of RL agents rather than simply looking at their specified reward function.

3) *Importance of TLNET Components:* Finally, the ablation study results shown in Table III show that filtering, regularization, and pruning are all important to the performance of TLNET. Removing predicate filtering notably reduced conciseness (by 27.2%) and consistency (by 46.1%). Removing regularization decreased conciseness (by 2.94%) and

TABLE III
ABLATION STUDY OF TLNET IN THE CTF CAPTURE SCENARIO.

Metrics	Full	No Filter	No Regularization	No Pruning
Conciseness	0.408	0.289	0.396	0.147
Consistency	0.325	0.175	0.233	0.2
Strictness	0.117	0.106	0.117	0.063
Accuracy	0.951	0.947	0.954	0.776

significantly reduced consistency (by 28.3%) with marginal accuracy improvement. Finally, removing the pruning step nearly tripled conciseness and halved strictness.

V. CONCLUSION

We introduce a neuro-symbolic framework, based on the TLNET architecture, for generating wSTL explanations of robot policies. Our approach generates easy-to-understand explanations through predicate filtering, loss regularization, and weight pruning. To assess explanation quality beyond classification metrics, we also propose explainability metrics—conciseness, consistency, and strictness. Experiments in three simulated robotic environments show that our method produces explanations that better capture these metrics while retaining high classification accuracy. By bridging neural network learning and formal logic-based explanations, our work advances explainability in complex robotic applications, with future directions including more expressive wSTL structures, human-in-the-loop refinement, and explainability-by-design policy optimization.

REFERENCES

- [1] S. Milani, N. Topin, M. Veloso, and F. Fang, “Explainable Reinforcement Learning: A Survey and Comparative Review,” *ACM Comput. Surv.*, vol. 56, no. 7, pp. 168:1–168:36, 2024.
- [2] R. Dwivedi, D. Dave, H. Naik, S. Singhal, R. Omer, P. Patel, B. Qian, Z. Wen, T. Shah, G. Morgan, and R. Ranjan, “Explainable AI (XAI): Core Ideas, Techniques, and Solutions,” *ACM Comput. Surv.*, vol. 55, no. 9, pp. 194:1–194:33, 2023.
- [3] O. Bastani, Y. Pu, and A. Solar-Lezama, “Verifiable reinforcement learning via policy extraction,” in *Proc. 32nd Int. Conf. Neural Inf. Process. Syst.*, Dec. 2018, pp. 2499–2509.
- [4] A. Iucci, A. Hata, A. Terra, R. Inam, and I. Leite, “Explainable Reinforcement Learning for Human-Robot Collaboration,” in *2021 20th Int. Conf. Advanced Robot.*, Feb. 2021, pp. 927–934.
- [5] E. M. Kenny, M. Tucker, and J. Shah, “Towards Interpretable Deep Reinforcement Learning with Human-Friendly Prototypes,” in *The 11th Int. Conf. Learn. Representations*, Sept. 2022.
- [6] M. Landajuela, B. K. Petersen, S. Kim, C. P. Santiago, R. Glatt, N. Mundhenk, J. F. Pettit, and D. Faissol, “Discovering symbolic policies with deep reinforcement learning,” in *Proc. 38th Int. Conf. Mach. Learn.*, July 2021, pp. 5979–5989.
- [7] A. Mott, D. Zoran, M. Chrzanowski, D. Wierstra, and D. J. Rezende, “Towards interpretable reinforcement learning using attention augmented agents,” in *Proc. 33rd Int. Conf. Neural Inf. Process. Syst.*, Dec. 2019, no. 1107, pp. 12 360–12 369.
- [8] N. Puri, S. Verma, P. Gupta, D. Kayastha, S. Deshmukh, B. Krishnamurthy, and S. Singh, “Explain Your Move: Understanding Agent Actions Using Specific and Relevant Feature Attribution,” in *Int. Conf. Learn. Representations*, Sept. 2019.
- [9] Y. Fukuchi, M. Osawa, H. Yamakawa, and M. Imai, “Explaining Intelligent Agent’s Future Motion on Basis of Vocabulary Learning With Human Goal Inference,” *IEEE Access*, vol. 10, pp. 54 336–54 347, 2022.
- [10] L. Trigg, B. Morgan, A. Stringer, L. Schley, and D. F. Hougen, “Natural Language Explanation for Autonomous Navigation,” in *AIAA DATC/IEEE 43rd Digit. Avionics Syst. Conf.*, Sept. 2024, pp. 1–9.
- [11] D. Das, S. Chernova, and B. Kim, “State2Explanation: Concept-Based Explanations to Benefit Agent Learning and User Understanding,” in *Thirty-Seventh Conf. on Neural Inf. Process. Syst.*, Nov. 2023.
- [12] I. Buzhinsky, “Formalization of natural language requirements into temporal logics: a survey,” in *2019 IEEE 17th Int. Conf. on Industrial Informatics (INDIN)*, vol. 1, July 2019, pp. 400–406.
- [13] M. Cosler, C. Hahn, D. Mendoza, F. Schmitt, and C. Trippel, “nl2spec: Interactively Translating Unstructured Natural Language to Temporal Logics with Large Language Models,” in *Comput. Aided Verification*, 2023, pp. 383–396.
- [14] E. Bartocci, C. Mateis, E. Nesterini, and D. Nickovic, “Survey on mining signal temporal logic specifications,” *Information and Computation*, vol. 289, p. 104957, Nov. 2022.
- [15] B. P. Bhuyan, A. Ramdane-Cherif, R. Tomar, and T. P. Singh, “Neuro-symbolic artificial intelligence: a survey,” *Neural Computing and Applications*, vol. 36, no. 21, pp. 12 809–12 844, July 2024.
- [16] J.-R. Gaglione, D. Neider, R. Roy, U. Topcu, and Z. Xu, “Learning Linear Temporal Properties from Noisy Data: A MaxSAT-Based Approach,” in *Automat. Technol. Verification Anal.*, 2021, pp. 74–90.
- [17] G. Bombara and C. Belta, “Offline and Online Learning of Signal Temporal Logic Formulae Using Decision Trees,” *ACM Trans. Cyber-Phys. Syst.*, vol. 5, no. 3, pp. 22:1–22:23, 2021.
- [18] E. Aasi, C. I. Vasile, M. Bahreinian, and C. Belta, “Classification of Time-Series Data Using Boosted Decision Trees,” in *2022 IEEE/RSJ Int. Conf. Intell. Robots Syst.*, Oct. 2022, pp. 1263–1268.
- [19] M. Yuasa, H. T. Tran, and R. S. Sreenivas, “On Generating Explanations for Reinforcement Learning Policies: An Empirical Study,” *IEEE Control Syst. Lett.*, vol. 8, pp. 3027–3032, 2024.
- [20] N. Mehdipour, C.-I. Vasile, and C. Belta, “Specifying User Preferences Using Weighted Signal Temporal Logic,” *IEEE Control Syst. Lett.*, vol. 5, no. 6, pp. 2006–2011, Feb. 2021.
- [21] R. Yan, A. Julius, M. Chang, A. Fokoue, T. Ma, and R. Uceda-Sosa, “STONE: Signal Temporal Logic Neural Network for Time Series Classification,” in *2021 Int. Conf. Data Mining Workshops*, Dec. 2021, pp. 778–787.
- [22] R. Tian, M. Cui, and G. Chen, “A Neural-Symbolic Network for Interpretable Fault Diagnosis of Rolling Element Bearings Based on Temporal Logic,” *IEEE Trans. Instrum. Meas.*, vol. 73, pp. 1–14, 2024.
- [23] N. Baharisangari, K. Hirota, R. Yan, A. Julius, and Z. Xu, “Weighted Graph-Based Signal Temporal Logic Inference Using Neural Networks,” *IEEE Control Syst. Lett.*, vol. 6, pp. 2096–2101, 2022.
- [24] R. Yan, T. Ma, A. Fokoue, M. Chang, and A. Julius, “Neuro-symbolic Models for Interpretable Time Series Classification using Temporal Logic Description,” in *2022 IEEE Int. Conf. Data Mining*, Jan. 2022, pp. 618–627.
- [25] D. Li, M. Cai, C.-I. Vasile, and R. Tron, “Learning Signal Temporal Logic through Neural Network for Interpretable Classification,” in *2023 American Control Conf. (ACC)*, May 2023, pp. 1907–1914.
- [26] X. Li, Z. Serlin, G. Yang, and C. Belta, “A formal methods approach to interpretable reinforcement learning for robotic planning,” *Science Robotics*, vol. 4, no. 37, p. eaay6276, Dec. 2019.
- [27] R. de Lazcano, K. Andreas, J. J. Tai, S. R. Lee, and J. Terry, “Gymnasium robotics,” 2024. [Online]. Available: <http://github.com/Farama-Foundation/Gymnasium-Robotics>
- [28] J. Ji, B. Zhang, J. Zhou, X. Pan, W. Huang, R. Sun, Y. Geng, Y. Zhong, J. Dai, and Y. Yang, “Safety Gymnasium: A Unified Safe Reinforcement Learning Benchmark,” *Advances in Neural Inf. Process. Syst.*, vol. 36, pp. 18 964–18 993, Dec. 2023.
- [29] A. Raffin, A. Hill, A. Gleave, A. Kanervisto, M. Ernestus, and N. Dormann, “Stable-Baselines3: Reliable Reinforcement Learning Implementations,” *J. Mach. Learn. Res.*, vol. 22, no. 268, pp. 1–8, 2021.
- [30] J. Schulman, F. Wolski, P. Dhariwal, A. Radford, and O. Klimov, “Proximal Policy Optimization Algorithms,” Aug. 2017, arXiv:1707.06347 [cs].
- [31] T. Haarnoja, A. Zhou, P. Abbeel, and S. Levine, “Soft Actor-Critic: Off-Policy Maximum Entropy Deep Reinforcement Learning with a Stochastic Actor,” in *Proc. 35th Int. Conf. Machine Learn.*, July 2018, pp. 1861–1870.
- [32] M. Andrychowicz, F. Wolski, A. Ray, J. Schneider, R. Fong, P. Welinder, B. McGrew, J. Tobin, O. Pieter Abbeel, and W. Zaremba, “Hindsight Experience Replay,” in *Advances Neural Inf. Process. Syst.*, vol. 30, 2017.
- [33] A. Raffin, “RL Baselines3 Zoo,” <https://github.com/DLR-RM/rl-baselines3-zoo>, 2020, GitHub repository.